FULL PAPER

Dalton
www.rsc.org/dalton

Potentiometric, spectroscopic and antioxidant activity studies of SOD mimics containing carnosine †

Raffaele P. Bonomo,[a] Valeria Bruno,[b,c] Enrico Conte,[a] Guido De Guidi,[a] Diego La Mendola,[d] Giuseppe Maccarrone,[a] Ferdinando Nicoletti,[b,c] Enrico Rizzarelli,*[a,d] Salvatore Sortino[a] and Graziella Vecchio[a]

[a] *Dipartimento di Scienze Chimiche, Università di Catania, Viale A. Doria 6, 95125 Catania, Italy. E-mail: erizzarelli@unict.it*

[b] *Dipartimento di Fisiologia Umana e Farmacologia, Università di Roma "La Sapienza", Piazzale A. Moro 5, 00185 Roma, Italy*

[c] *Dipartimento di Neuroscienze, I. N. M. Neuromed, Località Camerelle, 86077 Pozzilli, Italy*

[d] *Istituto di Biostrutture e Bioimmagini-Sez. di Catania, CNR, Viale A. Doria 6, 95125 Catania, Italy*

Received 16th July 2003, Accepted 9th September 2003
First published as an Advance Article on the web 25th September 2003

Stability constant values and bonding details of the copper(II) complexes of the β-cyclodextrin functionalized with the carnosine dipeptide (β-alanyl-L-histidine) at its narrow (CDAH6) or at its wide (CDAH3) rim were determined in aqueous solution. The potentiometric and spectroscopic data (UV-vis, CD and EPR) show that the involvement of a secondary OH group induces drastic differences in the coordination properties of CDAH3, in comparison with those of CDAH6. Direct and indirect assays were carried out showing that the copper(II) complexes with the two cyclodextrin derivatives are SOD-mimics with high catalytic activity. In addition the complex species are scavenger compounds towards $^{\bullet}OH$ radicals, giving rise to a particular kind of copper(II) complexes with a combined activity against two toxic radical species, $O_2^{\bullet -}$ and $^{\bullet}OH$. The cyclodextrin moiety contributes to the scavenger activity, without damaging the cellular membranes of neuronal and red blood cells.

Introduction

Carnosine, a naturally-occurring dipeptide (β-alanyl-L-histidine) was described in 1900 by Gulewitsch and Amiradzi.[1] Present in several mammalian tissues, including skeletal muscle and the brain (up to 20 mM in humans),[2–7] carnosine is synthesized by carnosine synthetase[8] from its component amino acids and it is degraded by carnosinase[9] and not readily attacked by specific peptidases.[10] Many homeostatic and protective functions have been described,[11] including antioxidant and free radical scavenging properties.[12,13] It has also been suggested that carnosine may play a role in copper metabolism *in vivo* and its chelating ability to copper(II) has been invoked to explain partly its protective activity against the copper-mediated neurotoxicity of neurons and other biomolecular targets,[14,15] but the chelation of the copper(II) is not detrimental to the scavenging ability of the dipeptide.[16]

Recent evidence suggests that carnosine can inhibit the aggregation of amyloid peptide[17] and that the toxic effects of amyloid peptide can be prevented or reduced by carnosine.[18] However, exogenous carnosine entering the organism intravenously, intraperitoneally, with food or topically to the eye, is not accumulated by the tissues but is excreted in the urine or destroyed by carnosinase, present in blood plasma, liver, kidney, brain and other tissues except muscle.[19,20] More recently, *N*-α-acetylcarnosine has been proposed as a prodrug for L-carnosine, showing a digestion rate lower than that of carnosine.[21]

β-Cyclodextrin (β-CD) derivatives have been synthesized to be used as drug carriers both as inclusion complexes and as functionalized derivatives. Recently, biological peptides have been grafted onto CDs both to increase their solubility and to reduce their enzymatic digestion rate with proteases.[22,23] With this in mind, some carnosine-containing β-CDs have been synthesized and their ability to scavenge $^{\bullet}OH$ radicals has been determined.[24]

This paper reports a complete characterization of two previously synthesized carnosine derivatives, the 6-deoxy-6-(β-alanylhistidyl)-β-cyclodextrin (CDAH6) and the $3^A(R)$-deoxy-$3^A(R)$-(β-alanylhistidyl)-$2^A(S)$-β-cyclodextrin (CDAH3). The different conformations of the CD–carnosine derivatives, obtained by NMR measurements at different pHs, were correlated with the proton complex constant values, determined by means of potentiometric measurements. EMF measurements were also carried out to obtain the copper(II) complex stability constants at 25 °C and $I = 0.1$ mol dm^{-3} (KNO_3). The different metal complex species were characterized by means of UV-vis, CD and EPR spectroscopic measurements, pointing out the role played by the OH groups of the wide rim of the CD moiety. Direct and indirect assays were carried out to prove the catalytic SOD-like and $^{\bullet}OH$ scavenger activities of the species existing in the experimental conditions of the *in vitro* assays. The speciation, obtained on the basis of the stability constant values, allows correlation of the antioxidant activities with the coordination environment of the metal complexes and with the conformation of the ligands. The protective effects of the copper(II) complexes with CD–carnosine derivatives were determined in the presence of different kind of cells, showing that CD moiety is not toxic for the cellular membranes.

Experimental

Materials

β-Cyclodextrin was purchased from Fluka and carnosine from Sigma; anhydrous *N*,*N*-dimethylformamide was purchased from Aldrich. They were used without further purification. Thin Layer Chromatography (TLC) was carried out on silica gel plates (Merck 60-F254). CD derivatives were detected on TLC by UV and by the anisaldehyde test or by the Pauli test for the derivatives of carnosine. The synthesis of the ligands (purity higher than 99%) were carried out as reported elsewhere.[24]

† Electronic supplementary information (ESI) available: Tables S1–S5 and Figs. S1–S3: additional experimental and calculated data. See http://www.rsc.org/suppdata/dt/b3/b308168k/

DOI: 10.1039/b308168k

Copper(II) nitrate was prepared from copper(II) basic carbonate by adding a slight excess of HNO_3. The concentration of stock solutions was determined by EDTA titrations using murexide as indicator.[25] The excess HNO_3 was determined by Gran's method[26] and by the ACBA computer program.[27] Stock solutions of HNO_3 and KOH were standardized by titration with primary standard tris(hydroxymethyl)aminomethane (THAM) and potassium hydrogen phthalate, respectively. Potassium nitrate (Suprapur Merck) was used without further purification. All solutions were prepared with doubly distilled water. Ketoprofen (KPF) sodium salt dihydrate and superoxide dismutase (SOD) were obtained from Sigma. All reagents were of analytical grade, unless otherwise stated.

Phosphate-buffered saline (Suprapur Merck) (PBS, pH 7.4) consisted of a 1×10^{-2} mol dm^{-3} phosphate buffer and 0.135 mol dm^{-3} NaCl solution. Red blood cells (RBCs) were prepared from samples of out-of-date (not more than 15 days from the date stated) packed human erythrocytes, supplied by the local blood bank, by washing them 4 times with 10-fold volume of PBS, each time centrifuging the cells at 2500*g* for 15 min and carefully removing the supernatant. Erythrocytes from out of date packed cells gave reproducible results over many days.[28]

Spectroscopic measurements

^{1}H NMR spectra were recorded at 25 °C in D_2O at the native pH and after adding of the stoichiometric amount of DCl or of NaOD. The spectra were carried out with a Varian Inova 500 spectrometer at 499.883 MHz. The ^{1}H NMR spectra were obtained by using standard pulse programs from the Varian library. In all cases the length of 90° pulse was *ca*. 7 μs. 2D experiments were acquired using 1K data points, 256 increments and a relaxation delay of 1.2 s. T-ROESY spectra were obtained using a 300 ms spin-lock time. ^{13}C NMR spectra were recorded at 25 °C in D_2O with a Bruker AC-200 spectrometer at 50.9 MHz. DSS was used as external standard.

EPR spectra were recorded on a Bruker ER 200D X-band spectrometer driven by a Bruker ESP 3220 data system equipped with standard low-temperature apparatus. All spectra were recorded at 150 K using quartz tubes with 3 mm inner diameters. The microwave frequency was calibrated with the use of powdered DPPH samples (g = 2.0036), while the magnetic field was carefully measured during each spectrum scan by means of a Bruker gauss meter, type ER 035 M.

Solutions of $^{63}Cu(NO_3)_2$ (2 mmol dm^{-3}) and ligand in water–methanol (95 : 5), adjusted to the required pH, were used to record the EPR spectra. Solutions containing 10% in methanol were used in the presence of 1-adamantanol. For copper(II) complexes with CDAH3 as ligand the $g_\parallel$ and $A_\parallel$ values were taken directly from the experimental spectra. For CDAH6, the parallel spin-Hamiltonian parameters were calculated using the GNDIMER program, which uses the dipole–dipole as the only source of anisotropic coupling between the two copper ions.[29]

Electronic and CD spectra were recorded on a Hewlett-Packard HP 8452 spectrophotometer and a JASCO J-810 dichrograph, respectively. Calibration of the CD instrument was performed with a 0.06% solution of ammonium camphorsulfonate in water ($\Delta\varepsilon$ = 2.40 M^{-1} cm^{-1} at 290.5 nm). The spectral range between 200 and 700 nm was covered by using quartz cells of various path lengths. Dilution of the solution was therefore not required. Results are reported in terms of ε (molar adsorption coefficient) and $\Delta\varepsilon$ (molar CD coefficient) in M^{-1} cm^{-1}.

EMF Measurements

Potentiometric titrations were performed with a computer-controlled Metrohm digital pH meter (Model 654) and Hamilton digital dispenser (mod microlabm). The titration cell (2.5 ml) was thermostated at 25.0 ± 0.2 °C and all solutions were kept under an atmosphere of argon, which was bubbled through another solution at the same conditions of ionic strength and temperature. KOH solution was added through a Hamilton burette equipped with 0.25 or 0.50 cm^3 syringes. The combined microelectrode (ORION 9103SC) was calibrated on the pH = $-\log[H^+]$ scale by titrating HNO_3 with CO_2 free base. The ionic strength of all solutions was adjusted to 0.10 mol dm^{-3} (KNO_3). The analytical concentrations of Cu^{2+} were varied from 1.5×10^{-3} to 7.5×10^{-3} mol dm^{-3}. Four different ligand to metal ratios (between 2.7 : 1 and 1 : 1.5) were employed. Other details were as previously reported.[30]

Calculations of the electrode system, E° values and ligand purity were performed by the least-squares computer program ACBA.[27] The HNO_3 excess in metal stock solutions was determined by Gran's method.[26] Calculation of the formation constants of the copper(II) complexes were performed by means of the least-squares computer program SUPERQUAD.[31] The species distribution as a function of pH was obtained by using the computer program DISDI.[32]

Superoxide dismutase indirect assay

SOD-like activity was determined by the indirect method of Nitro Blue of Tetrazolium salt (NBT) reduction.[33] Solutions containing $Cu(NO_3)_2$ (10^{-5}–10^{-7} mol dm^{-3}) and the ligand in phosphate buffer (5×10^{-3} mol dm^{-3}, pH 7.4) were used. The ligand was used in a range of large ligand/metal ratios (from 1 : 1 to 1000 : 1). The superoxide anion was enzymatically generated by the xanthine–xanthine oxidase system and spectrophotometrically detected by monitoring the formation of the reduced reporter molecule which absorbs at 560 nm.

An appropriate amount of xanthine oxidase was added to 2 ml of reaction mixture (NBT 5×10^{-5} mol dm^{-3}, xanthine 5×10^{-5} mol dm^{-3}, in phosphate buffer 5×10^{-3} mol dm^{-3} at pH 7.4) in order to cause a $\Delta A_{560\ nm}$ min^{-1} of 0.024. This corresponds to an $O_2^{\bullet -}$ production rate of 1.1×10^{-6} mol dm^{-3} min^{-1}. The NBT reduction rate was measured in the presence and in the absence of the investigated complexes for 300 s. All measurements were carried out at 25 ± 0.2 °C using 1 × 1 cm thermostatted cuvettes. Urate production by xanthine oxidase was spectrophotometrically monitored at 298 nm, ruling out any inhibition of xanthine oxidase activity.

The I_{50} (the concentration which causes the 50% inhibition of NBT reduction) of copper(II) complexes at pH 7.4 was calculated.

Pulse radiolysis assay

Pulse radiolysis was performed by using electron pulses (≈20 ns duration) from the 12 MeV electron linear accelerator at the FRAE-CNR Institute in Bologna. The irradiations were carried out at room temperature, 22 ± 2 °C, on samples contained in Spectrosil cells of 2 cm optical path length. Solutions were protected from the analyzing light by means of a shutter and appropriate cutoff filters. The monitoring light source was a 450 W Xe arc lamp. The radiation dose per pulse was monitored by means of a charge collector placed behind the irradiation cell and calibrated with a N_2O-saturated solution containing 0.1 mol dm^{-3} HCO_2^- and 0.5×10^{-3} mol dm^{-3} methyl viologen (1,1′-dimethyl-4,4′-bipyridinium dication; MV^{2+}) using $G\varepsilon = 9.66 \times 10^{-4}$ m^2 J^{-1} at 602 nm.[34] G(X) represents the number of moles of species X formed or consumed per joule of energy absorbed by the system.

The radiolysis of water predominantly produces the species shown in eqn. (1) where the values in parentheses represent the yields expressed in terms of G-values (μmol J^{-1}).[35]

$$H_2O \longrightarrow e_{aq}^- (0.27),\ ^\bullet OH (0.28) \text{ and } H^\bullet (0.062),\ H_2 (0.047),\ H_2O_2 (0.073),\ H^+ (0.27) \quad (1)$$

Reaction of $O_2^{\bullet -}$ radical with Cu–CDAH3 and Cu–CDAH6. If the solutions are saturated with oxygen in the presence of

10^{-2} mol dm^{-3} formate ion, the following reactions take place in the irradiated solution:

$$e_{aq}^- + O_2 \longrightarrow O_2^{\bullet -} \quad (2)$$

$$H^\bullet + O_2 \longrightarrow HO_2^\bullet \quad (3)$$

$$HO_2^\bullet \leftrightharpoons H^+ + O_2^{\bullet -}: pK_a = 4.69 \quad (4)$$

$$^\bullet OH + HCOO^- \longrightarrow CO_2^{\bullet -} + H_2O \quad (5)$$

$$CO_2^{\bullet -} + O_2 \longrightarrow CO_2 + O_2^{\bullet -} \quad (6)$$

Under these experimental conditions the superoxide radical anion is generated within less than 1 μs after the pulse, with a yield of 0.61. Since the dose used was ≈16 Gy, the concentration of $O_2^{\bullet -}$ was ≈10^{-5} mol dm^{-3}. The characteristic absorption band of $O_2^{\bullet -}$ in the UV region[36] enables the direct measurements of its decay at 250 nm.

Reaction of $^\bullet$OH radicals with Cu–CDAH3 and Cu–CDAH6. Samples containing either Cu–CDAH3 or Cu–CDAH6 were irradiated after saturating the aqueous solutions with N_2O. Under these experimental conditions the e_{aq}^- are converted into $^\bullet$OH according to reaction (7)

$$e_{aq}^- + N_2O + H_2O \longrightarrow {}^\bullet OH + OH^- + N_2 \quad (7)$$

and the yield of this species increases to *ca*. 0.55. Since the dose used in our experiments was ≈16 Gy, the concentration of $^\bullet$OH generated is ≈10^{-5} mol dm^{-3}.

The error in catalytic constants is ±15%.

Photohemolysis assay

Irradiation for photohemolysis tests was performed using a Rayonet photochemical reactor equipped with eight "black light" phosphor lamps with an emission in the 310–390 nm range with a maximum at 350 nm. The incident photon flux on 3 ml of investigated sample in quartz cuvettes (optical length 1 cm) was 6×10^{15} quanta s^{-1}, which is of the same order as the solar fluence incident on skin. A "merry-go-round" irradiation apparatus was used to ensure that all parallel samples received equal radiation. The experimental procedures of irradiation and the light intensity measurements have previously been described.[37]

Photohemolysis experiments were carried out with red blood cell (RBC) suspensions in the presence of ketoprofen (KPF)-containing copper(II) nitrate (10^{-6}–10^{-7} mol dm^{-3}) and CD derivatives in a 2 : 1 ratio with respect to the copper(II) ion; the metal ion and the ligands were premixed. In all experiments, the KPF concentration was equal to 4×10^{-5} mol dm^{-3}, which corresponds to the value used in previous photosensitization experiments[38] and very close to blood serum KPF levels after oral administration.[39] After the addition of RBCs, the samples were irradiated using the UVA source previously described.

Photohemolysis experiments were carried out in PBS by measuring the decrease in the absorbance at 650 nm as a function of time, measured from the beginning of the irradiation (delayed hemolysis time), since the optical density due to scattering cells is linearly proportional to the number of intact RBCs.[40] All the photohemolysis values were obtained by analysis of a sigmoidal Boltzman fit.

Each series of tests was performed with aliquots from the same sample of blood. Results were expressed as a percentage of total hemolysis by comparison with a sample in which the cells had been completely hemolyzed by brief sonication. The irradiation time ranged between 5 and 10 min and the delayed semihemolysis times (t_{50}) were in the range 40–350 min. No lysis was observed during this time when cells were irradiated in the absence of the photosensitising drug and/or metal complexes or incubated with these compounds in the dark.

An absorbance of 0.5 corresponded to 3.3×10^6 cells ml^{-1}. From the ratio between the t_{50} values in the presence and in the absence of the copper(II) complexes a protection factor F was calculated. This factor is independent on the irradiation time and the use of different blood samples gave reproducible results. Further details can be found in previous papers.[37,41]

Exicitotoxicity assay

Mixed cortical cell cultures containing both neurons and astrocytes were prepared from fetal mice at 14–16 d of gestation, as described previously.[42] Cultures were kept at 37 °C in a humified 5% CO_2 atmosphere. After 3–5 d *in vitro*, non-neuronal cell division was halted by 1–3 d exposure to 10 μM cytosine-β-arabinoside, and cultures were shifted to a maintenance medium identical to plating medium but lacking fetal serum. Subsequent partial medium replacement was carried out twice a week. Only mature cultures (13–14 d *in vitro*) were used for the experiments.

Brief exposure to 1×10^{-4} mol dm^{-3} NMDA (10 min), in the presence or absence of ligands and respectively copper(II) complexes (all solutions 1×10^{-4} mol dm^{-3}), was carried out in mixed cortical cultures at room temperature in a HEPES-buffered salt solution containing (in mmol dm^{-3}): 120 NaCl, 5.4 KCl, 0.8 $MgCl_2$ 1.8 $CaCl_2$, 20 HEPES, 15 glucose. After 10 min (NMDA) the solutions were washed out, and cultures were incubated at 37 °C for the following 24 h in medium stock (MS) (MEM-Eagle's supplemented with 15.8×10^{-3} mol dm^{-3} $NaHCO_3$ and glucose $<25 \times 10^{-3}$ mol dm^{-3}). At the end of the incubation, neuronal degeneration was examined by phase-contrast microscopy and quantified after staining with trypan blue. Stained neurons were counted from three random fields per well.[42]

Results and discussion

Conformational analysis of unprotonated and protonated CDAH3 and CDAH6 species

CDAH3. The NMR spectra of CDAH3, in the native zwitterionic form have previously been described.[24] A rigid disposition of the chain, due to the self-inclusion of the imidazole residue, has been found. At basic pH, the CH_2 protons beta to the amino group, diastereotopic at pH 7, became equivalent and appear as a triplet at 2.32 ppm. The α-CH_2 protons remain diastereotopic at 2.62 and at 2.79 ppm. The evident up-field shift of the ethylenic protons is due to the deprotonation of the NH group. The signals due to the 3A and 4A are up-field shifted at 2.73 and at 3.91 ppm as a consequence of deprotonation. The molecule becomes more asymmetric and six groups of signals appear in the H-1 region. The coupling constant values between H-1A and H-2A ($J_{1A,2A}$ = 7 Hz) and between 2A and 3A ($J_{2A,3A}$ = 10 Hz) indicated that 1A, 2A, 3A protons are axial. Furthermore, the coupling constant value for H-3A with H-4A ($J_{3A,4A}$ = 3.5 Hz) indicated an equatorial orientation of the H-4A proton. These data, compared with the calculated J for D-glucopyranosid rings, suggest that the altrose residue is in $^1C_4 \leftrightharpoons {}^0S_2$ conformational equilibrium shifted towards the $^1C_4$ conformation, as typically described for this class of compounds.[43–46] The involvement of the NH in the H-bond formation, in a similar way of the native CD, can be hypothesized as found for similar CD-derivatives.[47,48] The diastereotopicity of the protons of the ethylenic chain of carnosine, especially of the α-CH_2, suggesting the rigidity of the chain, is in keeping with this hypothesis. The ROESY spectra show cross-peaks between

the H-2 and H-5 protons of imidazole and the H-3,5,6 region and between H-2 and H-5A, as in the case of the spectra of the zwitterionic form. This indicates the self inclusion of imidazole in the cavity, thus the protonation of the amino group does not influence the interaction of the heterocyclic ring with the CD hydrophobic cavity.

At basic pH and at native pH, where the self-inclusion of imidazole ring is observed, the addition of 1-adamantanol (1-ad) induces evident modification to the spectra, especially in the region of the chain and the altrose unit. It is evident that the CH_2 protons beta to the amino group are not diastereotopic, differently than in the CDAH3 alone at the same pH, in keeping with the freedom of the chain.

The ROESY spectra indicate that the 1-ad is included in the cavity, replacing the imidazole ring. The presence of 1-adamantanol also induces some modification of the chemical shifts of the altroside residue. The H-3A and H-5A protons are at 2.73 ppm and at 3.98 ppm. The H-5A is up-field shifted by as much as 0.22 ppm, suggesting an orientation of the 5A inside the cavity rather than outside as in a $^1C_4$ conformation. The $J_{3A,4A}$ and $J_{4A,5A}$ is 5 Hz, higher than the CDAH3 without 1-ad, while the $J_{1A,2A}$ is not changed (7 Hz). This modification could suggest a different contribution of the conformers in the equilibrium $^1C_4 \leftrightarrows {}^0S_2$.[44]

The conformational modification of the altrose residue, induced by a guest, could modify the coordination ability and the complexing features of the set of donor atoms involved in the complexation with the metal ion, as previously reported for similar systems.[47,48]

The ^{1}H NMR spectra, at acid pH, show the shift of some protons. The ethylenic protons are further down field shifted because the amino group is completely protonated. The imidazole protons are down shifted in keeping with the protonation of imidazole nitrogen. The coupling constant value between H-1A and H-2A ($J_{1A,2A}$ = 6.5 Hz) indicates that 1A, 2A protons are axial, suggesting the $^1C_4 \leftrightarrows {}^0S_2$ conformational equilibrium exists but a larger amount of $^0S_2$ can be hypothesized in comparison with the unprotonated forms, similar to the inclusion complexes with 1-ad. The ROESY spectra of the CDAH3 at acid pH, do not show NOE-correlation between the imidazole ring and the CD protons. This indicates that the self inclusion of the heterocyclic ring is unfavored by the protonation of imidazole residue.

CDAH6. The NMR spectra, at native pH, have previously been discussed,[24] excluding the inclusion of imidazole in the cavity. The ^{1}H NMR spectra of CDAH6 in the presence of 1-ad were now carried out and no evident modification was observed.

At basic pH, the ligand is deprotonated and an evident downfield of 5A at 3.88 ppm and of 6A at 2.91 and 2.68 ppm is observed. Also the ethylenic chain protons are shifted up-field, especially the α-CH_2 protons. This shift is in keeping with the deprotonation of the amino group. The ROESY spectra suggest that no interaction of the chain with the cavity exists, differently from the CDAH3. The high multiplicity of the signal due to protons of the ethylenic chain, especially of the β protons to the amino group, could suggest the involvement of the peptide chain or of the imidazole ring in the hydrogen bonding formation with the OH groups of narrow rim. The spectra, at acid pH, show the downfield shift of the imidazole ring protons, in keeping with the protonation of imidazole. The β-CH_2 and α-CH_2 are now evidently diastereotopic suggesting that the protonation of imidazole ring seems to induce the rigidity of the chain. The ROESY spectra do not show NOE peaks between the chain and the H-3 and H-5 CD protons. This stiffening is not due to the self-inclusion of carnosine chain. Thus the protonated imidazole could interact more than the unprotonated form with the 6-OH rim forming hydrogen bonds as reported for similar systems.[49,50]

Table 1 Stability constant values for proton complex formation of AH, CDAH6 and CDAH3 at 25 °C and I = 0.10 mol dm^{-3} (KNO_3) (3σ in parentheses)

Equilibrium	log K
$AH^- + H^+ \rightleftarrows AH$	2.57(1)
$AH + H^+ \rightleftarrows AH(H)^+$	6.78(1)
$AH(H)^+ + H^+ \rightleftarrows AH(H)_2^{2+}$	9.40(1)
$CDAH6^- + H^+ \rightleftarrows CDAH6$	2.66(3)
$CDAH6^- + H^+ \rightleftarrows CDAH6(H)^+$	6.60(2)
$CDAH6(H)^+ + H^+ \rightleftarrows CDAH6(H)_2^{2+}$	7.69(2)
$CDAH3^- + H^+ \rightleftarrows CDAH3$	2.62(1)
$CDAH3 + H^+ \rightleftarrows CDAH3(H)^+$	6.47(2)
$CDAH3(H)^+ + H^+ \rightleftarrows CDAH3(H)_2^{2+}$	7.47(2)

Proton and copper(II) complexes: formation and bonding details

The formation reaction equilibria of the ligands with protons and copper(II) ions are given in eqn. (8), where L is the anion form of CDAH6 or CDAH3 (for the sake of clarity, charges on the copper(II) complexes have been omitted)

$$m\,Cu^{2+} + l\,L + h\,H \leftrightarrows Cu_mL_lH_h \quad (8)$$

The stability constant β_{mlh} is defined in eqn. (9)

$$\beta_{mlh} = [Cu_mL_lH_h]/[Cu]^m[L]^l[H]^h \quad (9)$$

Analysis of the titration data for CDAH6 and CDAH3, in the absence of copper(II), provides the formation constants for amino and imidazole nitrogen protonation as well as for carboxylate group (eqns. (10)–(12))

$$L^- + H^+ \leftrightarrows HL \quad (10)$$

$$HL + H^+ \leftrightarrows H_2L^+ \quad (11)$$

$$H_2L^+ + H^+ \leftrightarrows H_3L^{2+} \quad (12)$$

The proton complex formation constants, determined in this study, are given in Table 1 together with those found for carnosine (AH).

The equilibria necessary to fit the experimental titration curves for the solutions of copper(II) complexes formed with the CDAH ligands under study are given in eqns. (13)–(16).

$$Cu^{2+} + HL \leftrightarrows [CuLH]^{2+} \quad (13)$$

$$Cu^{2+} + L^- \leftrightarrows [CuL]^+ \quad (14)$$

$$Cu^{2+} + L^- \leftrightarrows [CuLH_{-1}] + H^+ \quad (15)$$

$$2\,Cu^{2+} + 2\,L^- \leftrightarrows [Cu_2L_2H_{-2}] + 2\,H^+ \quad (16)$$

Two additional equilibria were needed for CDAH3 (eqns. (17) and (18))

$$Cu^{2+} + 2\,L^- \leftrightarrows [CuL_2] \quad (17)$$

$$Cu^{2+} + L^- \leftrightarrows [CuLH_{-2}]^- + 2\,H^+ \quad (18)$$

the $[CuL_2]$ complex being a minor species.

The stability constant values of the copper(II) complexes of CDAH6, CDAH3 and AH are reported in Table 2.

The attachment of carnosine to the β-CD changes significantly the protonation constants of the amine nitrogen of the two isomers. Their log K values are nearly 2 logarithmic units lower than the log K value pertinent to the amino group of AH. Comparing the basicity of the histidine imidazole nitrogens,

Table 2 Stability constant values for copper(II) complexes of AH, CDAH6 and CDAH3 at 25 °C and $I = 0.10$ mol dm^{-3} (KNO_3) (3σ in parentheses)

Equilibrium	$\log\beta$
$Cu^{2+} + AH \rightleftarrows [Cu(AH)]^{2+}$	13.54(3)
$Cu^{2+} + AH^{-} \rightleftarrows [Cu(AH)]^{+}$	8.49(5)
$Cu^{2+} + AH^{-} \rightleftarrows [Cu(AH)(H_{-1})] + H^{+}$	2.98(5)
$2Cu^{2+} + 2AH^{-} \rightleftarrows [Cu_2(AH)_2(H_{-2})] + 2H^{+}$	8.06(6)
$2Cu^{2+} + AH^{-} \rightleftarrows [Cu_2(AH)(H_{-1})]^{2+} + H^{+}$	5.35(8)
$Cu^{2+} + CDAH6 \rightleftarrows [Cu(CDAH6)]^{2+}$	11.58(2)
$Cu^{2+} + CDAH6^{-} \rightleftarrows [Cu(CDAH6)]^{+}$	6.92(2)
$Cu^{2+} + CDAH6^{-} \rightleftarrows [Cu(CDAH6)(H_{-1})] + H^{+}$	1.3(2)
$2Cu^{2+} + 2CDAH6^{-} \rightleftarrows [Cu_2(CDAH6)_2(H_{-2})] + 2H^{+}$	6.33(3)
$Cu^{2+} + CDAH3 \rightleftarrows [Cu(CDAH3)]^{2+}$	11.68(1)
$Cu^{2+} + CDAH3^{-} \rightleftarrows [Cu(CDAH3)]^{+}$	8.33(1)
$Cu^{2+} + 2CDAH3^{-} \rightleftarrows [Cu(CDAH3)_2]$	12.73(5)
$Cu^{2+} + CDAH3^{-} \rightleftarrows [Cu(CDAH3)(H_{-1})] + H^{+}$	2.83(2)
$2Cu^{2+} + 2CDAH3^{-} \rightleftarrows [Cu_2(CDAH3)_2(H_{-2})] + 2H^{+}$	7.77(3)
$Cu^{2+} + CDAH3^{-} \rightleftarrows [Cu(CDAH3)(H_{-2})]^{-} + 2H^{+}$	−3.95(2)

slight differences can be observed, while the protonation constant values of the carboxylate groups do not show appreciable differences.

Thermodynamic data for proton complex formation of 3-functionalized CDs are scant. Previous data concerning the 3^A-deoxy-3^A-(2-methylaminopyridine)-$2^A(S)$,$3^A(R)$-β-cyclodextrin and the 3^A-[1-(2-amino)ethylamino]-3^A-deoxy-$2^A(S)$, $3^A(R)$-β-cyclodextrin showed $\log K$ values of amino group protonation lower than those of the parent molecules, the differences being higher than 2.5 logarithmic units.[47,48] In these functionalized β-CDs, the NH group replaces one 3-OH group usually involved in a network of H-bonding with the 2-OH group. The basicity decrease was attributed to this replacement, with the lone pair of amine nitrogen less available to interact with the hydrogen ion.[47,48] The NMR data of CDAH3 and previous results on similar systems,[45–48] at basic pH, indicate that also the amino group of carnosine is involved in the H-bonding network of the wide rim of the macrocycle, explaining the observed decrease of basicity. NMR spectra give information not only about the initial state of the molecule (unprotonated species), but also of its final state (protonated species). The protonated amine group appears to be involved in a non-covalent interaction. This contribution could counterbalance the less favorable initial state for the proton complex formation. The possible favorable (enthalpy) contribution should be compensated by the unfavorable (entropy) contribution due to the stiffening effect caused by the additional constraint. These opposite effects can explain the resulting basicity decrease.

NMR spectroscopy permitted the determination of the disposition of imidazole ring with respect to the cavity. At basic pH, the heterocyclic residue is inside the hydrophobic cavity. Due to the proton complex formation, the hydrophobic interaction is lost because the protonated imidazole leaves the cavity. The favorable contribution of the interaction of lone pair of imidazole nitrogen with the hydrogen ion is counterbalanced by the unfavorable contribution due to the removal of hydrophobic interaction with the cavity. The more or less equal contributions result in the slight decrease of imidazole basicity in CDAH3 in comparison to AH.

The decrease of the amino nitrogen basicity has been found for a number of aliphatic and heterocyclic diamines attached to the narrow rim of the β-CDs by means of the primary amine nitrogen.[51–54] The existence of an intrachain hydrogen bonding, the interaction with the primary OH groups of the rim as well as the steric and hydrophobic effects of the cavity have been used to explain the lower basicity in comparison with the parent ligands.[51–54] The NMR spectra of CDAH6 at different pH, do not give evidence of an intrachain interaction for the protonated and unprotonated amino nitrogen species. The basicity decrease of CDAH6 can be attributed to the breaking of a hydrogen bonding of the NH group with primary OH residue.

The $\log K$ value of the imidazole nitrogen protonation of CDAH6 is only 0.18 logarithmic units lower than that for the same protonation centre of AH. The NMR data show that the heterocyclic residue is placed on the rim, probably interacting with the OH residues of the rim. The protonation complex formation results in a stiffening of the chain. The two opposite effects can explain the slight variation of the $\log K$ value in comparison to the parent system.

Different species distribution profiles have been obtained for copper(II) complexes of CDAH6 and CDAH3 in the pH range studied (Figs. 1 and 2). At physiological pH, the main species of copper(II)–CDAH3 system is the monomeric $[Cu(CDAH3)H_{-2}]$ complex, while the prevailing complex of copper(II)–CDAH6 system is the dimeric $[Cu_2(CDAH6)_2H_{-2}]$ species. The copper(II) complexes of CDAH6 are less stable than the analogous species of AH. The differences in the stability constant values parallel the difference in the amine nitrogen protonation constants. Thus the same donor atoms are involved in the coordination to copper(II).

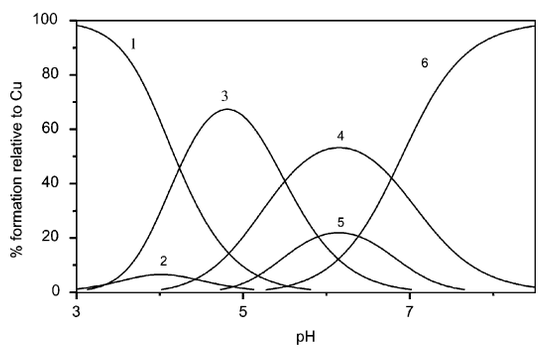

Fig. 1 Species distribution diagram for the copper(II)–CDAH3 system (1 : 1), C_L = 3.2 mmol dm^{-3}. 1 $[Cu^{2+}]$; 2 $[Cu(CDAH3)]^{2+}$; 3 $[Cu(CDAH3)]^{+}$; 4 $[Cu(CDAH3)H_{-1}]$; 5 $[Cu_2(CDAH3)_2H_{-2}]$; 6 $[Cu(CDAH3)H_{-2}]^{-}$.

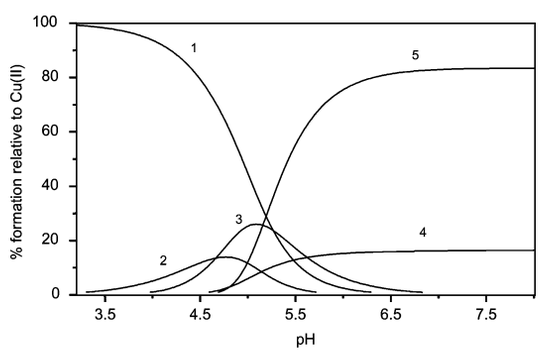

Fig. 2 Species distribution diagram for the copper(II)–CDAH6 system (1 : 1), C_L = 3.2 mmol dm^{-3}. 1 $[Cu^{2+}]$; 2 $[Cu(CDAH6)]^{2+}$; 3 $[Cu(CDAH6)]^{+}$; 4 $[Cu(CDAH6)H_{-1}]$; 5 $[Cu_2(CDAH6)_2H_{-2}]$.

The UV-vis and CD data, previously reported,[55] support this hypothesis that has been verified by the EPR parameters determined for the dimeric species. The spectrum of $[Cu_2(CDAH6)_2H_{-2}]$ complex, obtained at pH = 7, exhibits Δm = 1 transition resolved into a seven line pattern with apparent intensities of 1 : 2 : 3 : 4 : 3 : 2 : 1 and a peak-to-peak width of about 80 Gauss, this pattern arises from coupling of two copper(II) nuclei ($I = 3/2$) of a dimeric species and it is similar to the spectrum of the $[Cu_2(AH)_2H_{-2}]$ obtained in the same experimental conditions (see Table S1, ESI †).[56] On the basis of the magnetic parameters of $[Cu_2(AH)_2H_{-2}]$ species, the structure of this complex has been assessed:[57,58] each copper ion is chelated by amino and amide nitrogens and a carboxylate

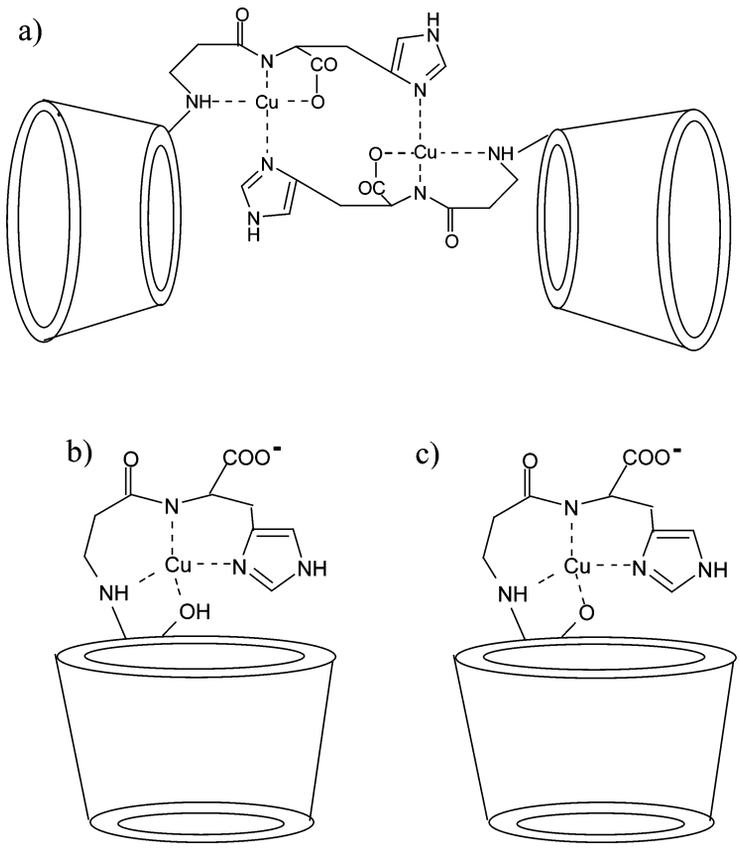

Fig. 3 Tentative structures of (a) the $[Cu_2(CDAH6)_2H_{-2}]$, (b) $[Cu(CDAH3)(H_{-1})]$ and (c) $[Cu(CDAH3)(H_{-2})]^-$ complexes.

oxygen of one ligand, with a coordination environment featuring two five- and six-membered chelate rings, while the imidazole 3-nitrogen of an other ligand molecule binds the copper(II) ion in the equatorial plane. A similar structure can be proposed for the analogous copper(II) complex with CDAH6 (Fig. 3(a))

The increase in $g_{\|}$ and the decrease in $A_{\|}$ values for the $[Cu_2(CDAH6)_2H_{-2}]$ complex, in comparison with the magnetic parameters of the $[Cu_2(AH)_2H_{-2}]$ species, indicate a decrease of the strength of the equatorial field. This is due both to the decreased basicity of the amino group in the complex of the β-CD derivative and to a slight distortion from a square planar geometry caused by the steric hindrance of the macrocyclic moiety. The imidazole rings bridging the two molecules probably causes a distortion of the coordination geometry (Fig. 3(a)). The previously reported red shift of the d–d transition band and the increase in the ε value[55] in comparison with the value pertinent to the copper(II) complex with the parent ligand,[59] support this conclusion.

The stability constant values for copper(II) complexes of the CDAH3 ligand are not different from those of the analogous species formed with AH. The different basicity of the amine group of CDAH3 is reflected only in the monoprotonated complex $[Cu(CDAH3)]^{2+}$ for which the involvement of the amine nitrogen results evident. To rationalize the trend observed for the other complexes, in comparison with those of the parent ligand, the coordination of additional donor atoms should be considered. The $\log K$ value of $[Cu(AH)]^+$ species, larger than that of other similar dipeptides, has been explained assuming that the coordination environment in the AH copper(II) complex was formed by a chelate ring between the amine nitrogen ed the deprotonated amide nitrogen, with the contemporary protonation of the histidine imidazole nitrogen.[58,59] The same donor atoms could be bound to copper(II) in the $[Cu(CDAH3)]^+$ complex, with the formation of one further chelate ring involving the rim OH group that is coplanar with the NH residue. This additional chelate ring formation can counterbalance the lesser tendency of amine group lone pair to interact with the metal center in comparison to that of the amine group of AH. The spectroscopic data are characterized by: (i) d–d transitions at 620 nm in the absorption spectrum (blue shifted in comparison to that of $[Cu(AH)]^+$ species with λ_{max} = 630 nm and ε = 38 M^{-1} cm^{-1}),[59] (ii) the CD spectrum which exhibits the charge transfer bands due to NH ⟶ Cu^{2+} (λ_{max} = 268 nm), N^- ⟶ Cu^{2+} (306 nm), OH ⟶ Cu^{2+} (λ_{max} = 500 nm); these spectroscopic data clearly support the coordination environment suggested on the basis of $\log K$ values (Table 2).

The $g_{\|}$ and $A_{\|}$ values (Table 3) are typical for a square planar geometry.[60] By adding 1-ad to a solution containing the $[Cu(CDAH3)]^+$ species (pH = 4.5), the EPR spectrum shows the signals typical of dimeric species (data not reported), that is the formation of $[Cu_2(CDAH3)_2H_{-2}]$ is favored. The guest substitutes the imidazole ring inside the cavity and the copper bond with the OH group is broken. The CD data are consistent with this change of the set of donor atoms. In fact, by adding the 1-adamantanol the OH ⟶ Cu^{2+} CT band at 500 disappears, and the CD bands in the visible region are similar to those found in the dimeric species of copper complex with AH, even if the λ_{max} = 603 nm (ε = 160) value is shifted to a longer wavelength.[61] The involvement of OH group in the copper(II) coordination group can be used to explain the similarity of $\log K$ values for the monodeprotonated species (Fig. 3(b)), while the $[Cu(CDAH3)H_{-2}]^-$ complex formation could be favored by the deprotonated OH group of the rim (Fig. 3(c)) or by the binding of an OH^- group from a water molecule.

In the pH range from 4.5 to 7.2, EPR spectra are characterized by the presence of more than one species, in accordance with the species distribution profile. As a consequence, all the spectroscopic data cannot be used to support the bonding details concerning the $[Cu(CDAH3)H_{-1}]$ and the $[Cu_2(CDAH3)_2H_{-2}]$ species. Above pH 8, the $[Cu(CDAH3)H_{-2}]^-$ complex formation predominates; the blue shift of the d–d transition in the absorption spectrum, the CT bands due to N_{im} ⟶ Cu^{2+} (λ_{max} = 240), NH ⟶ Cu^{2+} (λ_{max} = 277), N^- ⟶ Cu^{2+}

Table 3 Spectroscopic data for copper(II) complexes with CDAH3 ligand

Species	UV-vis λ/nm	ε/M^{-1} cm^{-1}	CD λ/nm	$\Delta\varepsilon$/M^{-1} cm^{-1}	EPR $g_{\parallel}$	$A_{\parallel} \times 10^{-4}$/cm^{-1}	pH
[Cu(CDAH3)]$^{+}$	205	15200	220	15.00			
	250	4000	268	1.40	2.235	196	4.5
	620	50	306	−0.78			
			500	−0.14			
			628	−0.39			
[Cu(CDAH3)]$^{+}$ + 1-ad	205	14800	220	18.50	–	–	4.5
	243	3900	268	1.95			
	638	60	339	0.31			
			622	0.22			
[Cu(CDAH3)H$_{-1}$]	–	–	–	–	–	–	–
[Cu(CDAH3)H$_{-2}$]$^{-}$			240	−1.60			
	595	100	277	1.90	2.225	188	8.7
			325	−0.50			
			480	−0.06			
			550	0.15			
			630	−0.19			
			760	0.10			
[Cu(CDAH3)H$_{-2}$]$^{-}$ + 1-ad			215	−1.57			
	595	100	241	−1.60	2.225	179	8.7
			280	1.35			
			329	−0.25			
			480	−0.06			
			540	0.05			
			620	−0.35			
			755	0.21			

(λ_{max} = 325) and $O^{-} \longrightarrow Cu^{2+}$ (λ_{max} = 480) as well as the lower $g_{\parallel}$ value indicate a tetragonal coordination geometry with a set of donor atoms in the equatorial plane constituted by three nitrogens (NH,N^{-},N_{im}) and a deprotonated OH group (Table 3). The involvement of the hydroxyl group of the β-CD rim is indicated by the fact that, while, up to neutral pH, the CT band disappears by adding the 1-ad (see Table S2, ESI †), at basic pH the CT band is not influenced; the ionized OH group gives rise to a tight bond with the copper(II) ion. The slight decrease of the hyperfine coupling constant ($A_{\parallel}$ =188) of [Cu(CDAH3)-H$_{-2}$]$^{-}$ complex in comparison to that of [Cu(CDAH3)]$^{+}$ is attributed to the strong bond of the negatively charged oxygen atom, with the disposition of imidazole nitrogen not completely coplanar with the other donor atoms. The inclusion of 1-ad in the β-CD cavity does not alter the number of donor atoms in the equatorial plane, in fact the $g_{\parallel}$ value is not modified. The $A_{\parallel}$ value decrease suggests a further distortion of the tetragonal geometry, while the possible involvement of the carboxylate group, perhaps in axial position, cannot be excluded.

Antioxidant activity

Low molecular weight mimics of SOD, containing transition metal ions, have been proposed[62,63] to overcome the limitations of the use of SOD enzymes as therapeutic agents and pharmaceutical tools.[62] Cellular permeability, longer half-life in the blood, potential for oral delivery and lower cost are the parameters in favor of the use of these compounds. However for these systems, the reliability of the method employed to determine their SOD activity is critical.

The SOD activity is principally measured by two methods: (i) the xanthine–xanthine oxidase system, in which $O_2^{\bullet -}$ is produced in the presence of oxygen and can be detected by reduction of cytochrome c or NBT;[33] and (ii) the pulse radiolysis method, in which controlled amounts of $O_2^{\bullet -}$ are rapidly produced in a solution containing the enzyme and its consumption can be followed by UV-vis spectroscopy.[36]

The first is an indirect method, as $O_2^{\bullet -}$ scavenging is detected by the decrease in the rate of cytochrome c or NBT reduction, while the second allows the direct measurement of $O_2^{\bullet -}$ consumption.

Table 4 SOD-like activity (Fridovich assay) for copper(II) complexes of functionalized cyclodextrins with carnosine (L/M = 1000, phosphate buffer 5 × 10^{-3} mol dm^{-3}, pH 7.4)

System	I_{50}[a] × 10^{7}/ mol dm^{-3}
SOD	0.14
Cu–CDAH6	2.4
Cu–CDAH3	4.3
Cu–AH	8.0
Cu–HPO_4	10.6

[a] The standard uncertainties are ± 20%.

In the indirect method, it is important to verify that there were not interferences: (i) the complex is not participating in the reaction with the detector molecule; (ii) it does not cause inhibition of the xanthine/xanthine oxidase production of $O_2^{\bullet -}$ or (iii) it does not react with H_2O_2 or oxygen products of self dismutation of $O_2^{\bullet -}$. Furthermore, the initial concentration of substrate could not be in large excess compared to that of the putative catalyst. This can lead to a false interpretation of catalytic activity, when there is a fast stoichiometric reaction with superoxide. On the contrary, the pulse radiolysis method allows precise measurements of the rate of dismutation of $O_2^{\bullet -}$.

In this context we report the antioxidant data of these copper(II) complexes by using both the indirect and direct methods and, in addition, some biological tests of the compounds including neurotoxicity *in vitro* and protection from photohemolysis.

Table 4 reports the SOD-like activity (expressed as I_{50}) of the copper(II) complexes of the two isomers determined by the indirect assay of NBT, and for comparison, the I_{50} values[64,65] pertinent to SOD and [Cu(HPO_4)].

Being aware that copper(II) forms labile complexes, the stability constant values here reported were used to obtain the concentrations of the different complex species present in the experimental conditions of the assay, according to the simulation approach previously reported.[41] At pH 7.4,

the [Cu(CDAH6)H_{-1}] complex is the main species for the Cu–CDAH6 system, while the [Cu(CDAH3)H_{-2}]$^{-}$ complex is the predominant species for the Cu–CDAH3 system (see Table S3, ESI †). The I_{50} value indicates that the copper(II) complex of the CDAH6 isomer is a SOD-like compound more active than the complex of the CDAH3 isomer, both being more active than the [Cu(HPO_4)] species and the [Cu(AH)H_{-1}] species.

The pulse radiolysis results agree with those of the indirect method. In the absence of copper(II) complexes the $O_2^{\bullet -}$ disappearance was slow and followed second-order kinetics with $k_1 = 10^5$ M^{-1} s^{-1}, in good agreement with the literature[36,66] (data not shown). On the contrary, in the presence of either Cu–CDAH3 or Cu–CDAH6 the reaction was clearly accelerated and the time profile for the $O_2^{\bullet -}$ decay (see Fig. S1A,B, ESI †) was described well by first-order kinetics with pseudo-first order rate constant, k_{obs}, of 1.25×10^4 and 2.10×10^3 s^{-1} for Cu–CDAH3 and Cu–CDAH6, respectively. By taking into account that the complexes concentration was lower than the initial $O_2^{\bullet -}$ concentration, it is clear that the both complexes were functioning in a catalytic fashion. This was corroborated by the fact that the kinetics observed did not change during repeated electron pulses on the same solution. The second order rate constants for Cu–CDAH3- and Cu–CDAH6-catalyzed disproportionation of superoxide anion were obtained by using eqn. (19), in according to that reported for other copper(II) complexes with catalytic activity.[67,68]

$$k_{cat} = k_{obs}/[\text{complex}] \quad (19)$$

The k_{cat} values were similar for both complexes being 2.3×10^9 and 1.9×10^9 M^{-1} s^{-1} for Cu–CDAH3 and Cu–CDAH6, respectively, and did not change significantly with the complex concentration. The results obtained account for a high superoxide dismutase activity of the two compounds. In fact, the related catalytic rate constants are of the same order of magnitude of the native enzyme.[69] Control experiments carried out with the ligands alone up to 10 μM ruled out any effects of these species on the rate of $O_2^{\bullet -}$ disappearance.

Fig. 4 shows the transient absorption spectrum taken 6 μs after the pulse and obtained after the reaction of $^{\bullet}$OH radicals with a 10^{-4} mol dm^{-3} aqueous solution of Cu–CDAH6. The spectrum is characterized by a relevant absorption below 280 nm, a shoulder around 300 nm and a better-defined band in the 350–400 nm region, respectively.

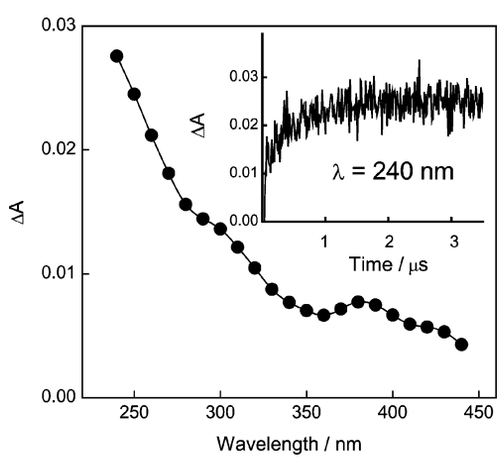

Fig. 4 Absorption spectrum obtained from the pulse radiolysis of N_2O-saturated 10^{-4} M solution of Cu–CDAH6 and taken 6 μs after the pulse. The inset shows the build-up monitored at 240 nm.

The shape of the spectrum obtained is very similar to that observed in the case of the pulse radiolysis of the ligand alone and reported in one of our recent investigations.[24] This study pointed out that both the imidazole and the β-CD subunits of CDAH6 behave as competitive sites for the scavenging of the $^{\bullet}$OH radicals. The close resemblance of the transient spectra of ligand and complex strongly suggests that also for the latter, the above scenario may come into play. This picture rules out, of course, any participation of the copper ion in the scavenging process. Actually, although Cu^{2+} could in principle quench the $^{\bullet}$OH radical with formation of Cu^{3+} species,[70,71] no spectral evidence accounting for the formation of these species was observed. This is in good agreement with what has been recently reported by Tamba and Torreggiani in the case of Cu(II) complexes with carnosine.[72]

The time profile showed in the inset of Fig. 4 is described fairly well by a first order fit with a pseudo-first order rate constant, $k_{obs} \sim 1 \times 10^6$ s^{-1}. A bimolecular quenching constant $k_{Cu-CDAH6} \sim 1 \times 10^{10}$ M^{-1} s^{-1}, related to the reaction of $^{\bullet}$OH with Cu–CDAH6, is obtained by using eqn. (20).

$$k_{(^{\bullet}OH + \text{complex})} = k_{obs}/[\text{complex}] \quad (20)$$

Such a value did not change significantly with the concentration of the complex, confirming that under these experimental conditions $^{\bullet}$OH radicals react almost exclusively with the quencher. Furthermore, it is interesting to note that this bimolecular quenching constant is basically similar to that reported for the ligand alone.[24]

Cu–CDAH3 exhibited spectral and kinetic features similar to Cu–CDAH6 (data not shown). Thus, the picture emerging from these results suggests that the chelation of Cu(II) is not detrimental for the scavenging ability of the ligand. However it was interesting to note that the metal ion tunes the relative distribution of $^{\bullet}$OH between the two different sites of attack (*i.e.* β-CD or imidazole). We gained direct insights about the amounts of the OH–imidazole adduct formed in each case by subtracting from the transient spectrum of the complex, the spectrum taken at the same dose and delay time in the case of a 10^{-4} mol dm^{-3} solution of β-CD alone.[24] The difference spectra obtained for the two complexes, with only the contribution of the resonance-stabilized radical formed at the level of the imidazole ring (see Fig. S2, ESI †), show (i) no drastic differences in the extinction coefficient of the OH-adducts for the two compounds, as reasonably expected, and (ii) the spectra are not affected by the ground state absorption of the complexes in the spectral region shown, so from the values of the ΔA obtained, one can readily note that the amount of the OH-imidazole adduct generated in the case of Cu–CDAH6 is about 40% lower than Cu–CDAH3. This finding is the opposite of what is found for the ligands themselves where the $^{\bullet}$OH exhibited higher preference for the imidazole ring of CDAH6 than the CDAH3.[24] Only in the case of the Cu–CDAH6 system, the dimeric species (40%) (see Table S4, ESI †) exists in the experimental conditions of the assay. As depicted in Fig. 3(a), the structural peculiarities of such dimer species are such that the direct attack of $^{\bullet}$OH radical on the imidazole centers could be significantly hindered due to steric factors. Furthermore it is also worth noting that the formation of imidazole–OH adduct for Cu–CDAH3 was about two-fold higher than the ligand alone. This finding is in good agreement with the exit of the imidazole ring from the CD cavity upon copper complexation both in the [Cu(CDAH3)H_{-1}] and the [Cu(CDAH3)H_{-2}]$^{-}$ species (Fig. 3(b) and (c)). In fact, we demonstrated that in CDAH3, the imidazole moiety is included within the CD cavity and thus it was remarkably hindered against $^{\bullet}$OH reaction.[24]

Photo- and neuro-protective activities

It is well known that Ketoprofen shows lytic action when irradiated in the presence of red blood cells (RBCs).[38,73] This photosensitizing activity can be explained on the basis of Ketoprofen photochemistry.[74] The photohemolysis results show that the complexes are able to reduce the KPF induced photosensitization processes in a dose-dependent way (see Fig. S3,

ESI †). Actually, KPF alone showed a t_{50} ranging between 40 and 90 min (depending on the irradiation time), whereas samples of KPF-containing the complexes show a lengthening of t_{50} up to values of about 300 min. At physiological pH, the predominant species for the two isomers are the $[Cu(CDAH6)H_{-1}]$ and the $[Cu(CDAH3)H_{-2}]^{-}$ complexes, respectively (see Table S5, ESI †). The protective activities of native SOD and $[Cu(HPO_4)]$ are reported for comparison. These latter data are in good agreement with those reported elsewhere,[41,64] excluding any effect of the cyclodextrin cavity both on the photodegradation and photosensitization mechanism of Ketoprofen, inasmuch as these effects, observed in unfunctionalized cyclodextrins, occur only at higher concentrations.[75,76]

Excitotoxicity refers to the ability of glutamate or related excitatory amino acids, like *N*-methyl-D-aspartate (NMDA), to mediate the death of central neurons after intense exposure.[77] Such excitotoxic neuronal death has been involved in the development of ischemic brain injury and the pathogenesis of other diseases, due to oxidative stress[78] and/or apoptosis.[79]

The addition of single ligands AH (100 nmol dm^{-3}–100 μmol dm^{-3}), CDAH6 (100 nmol dm^{-3}–100 μmol dm^{-3}), CDAH3 (100 nmol dm^{-3}–100 μmol dm^{-3}) or copper ions (1–100 μmol dm^{-3}) did not affect neuronal death induced by NMDA, while a good neuroprotective effect is observed after the addition of respective copper(II) complexes in an analytical concentration of 100 μmol dm^{-3} (Fig. 5). Again the CD moiety positively affects the protective effect of copper(II) complexes, excluding a damage to the cellular membrane. Considering the experimental error, the inhibition of neuronal death seems to be very similar for all complexes, this fact is due to the typology of assay where the role of the ROS is an important factor but not the only one.

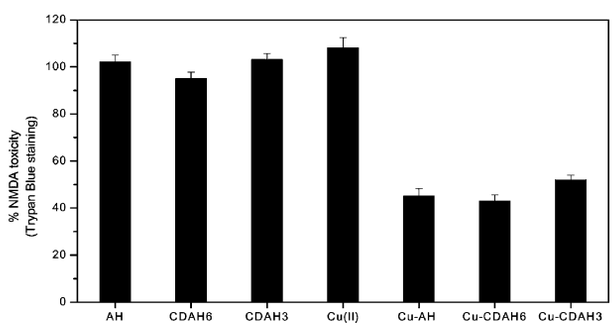

Fig. 5 Neuroprotective activity of ligands and copper(II) complexes in primary neuronal cultures in excitotoxicity assay. All solutions used are 1×10^{-4} mol dm^{-3}. Values represent mean ± SEM of 6–15 individual determinations. $p < 0.05$ (One-way ANOVA + Fisher's PLSD) *vs.* the control (NMDA alone).

Concluding remarks

Many metal complexes are known to react with and be reduced by superoxide or oxidized by its conjugate acid, but may nevertheless not act as a catalyst. Thus, the determination of true catalytic superoxide reactivity is critical to the claim that a complex is a SOD mimic.

Our data show that both the copper(II) complexes with the CD–carnosine derivatives are effective SOD-like compounds. In addition to their high catalytic activity, the copper(II) complexes also display a protective action against Ketoprofen induced photohemolysis and a neuroprotective effect with respect to the neuronal death induced by NMDA.

The usefulness of copper(II) complexes has been questioned because the metal ion forms labile complexes and the reduced species may react with H_2O_2, the product of dismutation of $O_2^{\bullet -}$, to generate hydroxyl radicals.[80] The CD–carnosine derivatives and their copper(II) complexes are scavengers of $^{\bullet}OH$ radicals and spectroscopic data allows the correlation of this activity with the structural features of the coordination compounds. In fact comparing the conformation of the side chain moiety in the free ligand (determined by NMR) with that of the metal bounded ligand (determined by EPR and CD), the tuning role of the metal ion in the distribution of the $^{\bullet}OH$ between the two different sites of attack (the β-CD and the imidazole residue) is brought to light.

The potentiometric data allows the species distribution profiles to be obtained in the experimental conditions of the different assays. The complex species survive in very dilute solutions and the prevailing metal complexes can be determined. This approach[81] can permit speculation about the structure–activity correlation of the two copper complexes formed by the two cyclodextrin isomers. During the catalytic process, the copper(II) ion of SOD abandons the square planar arrangement (with a water molecule in apical position) to assume a pseudotetrahedral stereochemistry, typical of Cu(I),[82,83] this raises the question about obtaining a SOD-mimic in which the ligand is able to provide a flexible coordination environment to facilitate the redox cycle Cu(II)/Cu(I), that is a ligand with a set of donors able to accommodate both the tetragonal copper(II) and the trigonal Cu(I) geometric requirements of the two ions. The $[Cu(CDAH6)H_{-1}]$ complex, the main species in the Fridovich, as well as in the photohemolysis assay, is more active in comparison with the $[Cu(CDAH3)H_{-2}]^{-1}$ complex, the prevailing species existing in the same experimental assays. Due to the coordination of the deprotonated OH group, the copper(II) ion experiences, in the complex with the CDAH3 derivative, a more rigid coordination plane in comparison to that in the complex with the CDAH6 isomer. Being aware that the donor atoms are different from those present in the enzyme, the stiffening in the copper(II) complex of the CDAH3 isomer can be proposed to be responsible for the lower catalytic activity compared to that of the copper(II) complex with CDAH6.

In conclusion, a combined thermodynamic and spectroscopy approach is useful not only to give a complete characterization of complex species in solution, but also to correlate their structural features with biological activities.

Acknowledgements

We wish to thank MIUR (Progetto FIRB 2001 RBNE01ZK8F) and the University of Catania for partial support. We wish to express our sincere thanks to Dr Q. G. Mulazzani for his inestimable help in the pulse radiolysis measurements and to Dr A. Martelli and A. Monti for their technical assistance.

References

1 W. Gulewitsch and S. Amiradzibi, *Ber. Dtsch. Chem. Ges.*, 1900, **33**, 1902.
2 K. G. Crush, *Comp. Biochem. Physiol.*, 1970, **34**, 3.
3 F. L. Margolis, *Science*, 1974, **184**, 909.
4 A. Neidle and J. Kandera, *Brain Res.*, 1974, **80**, 359.
5 J. E. Plowman and E. A. Close, *J. Sci. Food Agric.*, 1988, **45**, 69.
6 R. C. Harris, D. J. Marlin, M. Dunnet, D. Snow and E. Hultman, *Comp. Biochem. Physiol., A: Physiol.*, 1990, **97**, 249.
7 A. F. Mannion, P. M. Jokeman, M. Dunnet, R. C. Harris and P. L. Willan, *Eur. J. Appl. Physiol.*, 1992, **64**, 47.
8 M. R. Wood and P. Johnson, *Biochim. Biophys. Acta*, 1981, **662**, 138.
9 M. Teufel, V. Saudek, J. P. Ledig, A. Bernhard, S. Boulerand, A. Carreau, N. J. Cairns, C. Carter, D. J. Cowley, D. Duverger, A. J. Ganzhorn, C. Guenet, B. Heintzelmann, V. Laucher, C. Sauvage and T. Smirnova, *J. Biol. Chem.*, 2003, **278**, 6521, and references therein.
10 Y. Ito, M. Sugiura and S. Sawaki, *J. Biochem. (Tokyo)*, 1983, **94**, 871.
11 P. J. Quinn, A. A. Boldyrev and V. E. Formazuyc, *Mol. Aspects Med.*, 1992, **13**, 379.
12 R. Kohen, Y. Yamamoto, K. C. Cundy and B. Ames, *Proc. Natl. Acad. Sci. USA*, 1988, **85**, 3175.
13 M. Salim-Hanna, E. Lissi and L. Videla, *Free Radical Res. Commun.*, 1991, **14**, 263.
14 C. E. Brown and W. E. Antholine, *J. Phys. Chem.*, 1979, **83**, 3314.
15 M. S. Horning, L. J. Blakemore and P. Q. Trombley, *Brain Res.*, 2000, **852**, 56.

16 M. Tamba and A. Torreggiani, *Int. J. Radiat. Biol.*, 1999, **75**, 1177.
17 G. Munch, S. Mayer, J. Michaelis, A. R. Hipkiss, P. Riederer, R. Muller, A. Neumann, R. Schinzel and A. M. Cunnigham, *Biochim. Biophys. Acta*, 1997, **1360**, 17.
18 J. E. Preston, A. R. Hipkiss, D. T. Himsworth, I. A. Romero and J. N. Abbott, *Neurosci. Lett.*, 1998, **242**, 105.
19 J. F. Lenney, S. C. Peppers, C. M. Kucera-Orallo and R. P. George, *Biochem. J.*, 1985, **228**, 653.
20 M. C. Jackson, C. M. Kucera and J. F. Lenney, *Clin. Chim. Acta*, 1991, **196**, 193.
21 M. A. Babizhayev, V. N. Yermakova, Y. A. Semiletov and A. I. Deyev, *Biochemistry (Moscow)*, 2000, **65**, 588.
22 N. Schaschke, S. Fiori, E. Weyher, C. Escrieut, D. Fourmy, G. Muller and L. Moroder, *J. Am. Chem. Soc.*, 1998, **120**, 7030.
23 C. Pean, C. Creminon, A. Wijkhuisen, J. Grassi, P. Guenot, P. Jehan, J-P. Dalbiez, B. Perly and F. Djedaini-Pilard, *J. Chem. Soc., Perkin Trans. 2*, 2000, 853.
24 D. La Mendola, S. Sortino, G. Vecchio and E. Rizzarelli, *Helv. Chim. Acta*, 2002, **85**, 1633.
25 H. A. Flaschka, in *EDTA Titrations*, Pergamon Press, London, 1959.
26 G. Gran, *Analyst.*, 1952, **77**, 661.
27 G. Arena, E. Rizzarelli, S. Sammartano and C. Rigano, *Talanta*, 1979, **26**, 1.
28 P. Wang and J. Kagan, *Chemosphere*, 1989, **19**, 1345.
29 T. D. Smith and J. R. Pilbrow, *Coord. Chem. Rev.*, 1974, **13**, 173.
30 R. P. Bonomo, R. Calì, V. Cucinotta, G. Impellizzeri and E. Rizzarelli, *Inorg. Chem.*, 1986, **25**, 1641.
31 P. Gans, A. Sabatini and A. Vacca, *J. Chem. Soc., Dalton Trans.*, 1985, 1195.
32 R. Maggiore, S. Musumeci and S. Sammartano, *Talanta*, 1976, **23**, 43.
33 C. Beauchamp and I. Fridovich, *Anal. Biochem.*, 1971, **44**, 276.
34 Q. G. Mulazzani, M. D'Angelantonio, M. Venturi, M. Z. Hoffman and M. A. Rodgers, *J. Phys. Chem.*, 1986, **90**, 5347.
35 G. V. C. Buxton, L. Greenstock, W. P. Helman and A. B. Ross, *J. Phys. Chem.*, 1988, **17**, 513.
36 J. Rabani and S. O. Nielsen, *J. Phys. Chem.*, 1969, **73**, 3736.
37 G. Giammona, G. Pitarresi, V. Tomarchio, G. De Guidi and S. Giuffrida, *J. Control. Release*, 1998, **51**, 249.
38 Costanzo, L. L. G. De Guidi, G. Condorelli, A. Cambria and M. Famà, *Photochem. Photobiol*, 1989, **50**, 359.
39 A. C. Moffat, in *Clarke's Isolation and Identification of Drugs*, Pharmaceutical Press, London, 1986, p. 1032.
40 P. Valenzeno and J. W. Trank, *Photochem. Photobiol.*, 1985, **42**, 335.
41 L. L. Costanzo, G. De Guidi, S. Giuffrida, E. Rizzarelli and G. Vecchio, *J. Inorg. Biochem.*, 1993, **50**, 273.
42 V. Bruno, G. Battaglia, A. Copani, R. G. Giffard, G. Raciti, R. Raffaele, H. Shinozaki and F. Nicoletti, *Eur. J. Neurosci.*, 1995, **7**, 1906.
43 D. Q. Yuan, K. Otha and K. Fujita, *Chem. Commun.*, 1996, 821.
44 H. Ikeda, Y. Nagano, Y. Q. Du, T. Ikeda and F. Toda, *Tetrahedron Lett.*, 1990, **31**, 5045.
45 K. Fujita, K. Ohta, Y. Ikegami, H. Shimada, T. Tahara, Y. Nogami, T. Koga, K. Saito and T. Nakajima, *Tetrahedron Lett.*, 1994, **35**, 9577.
46 K. Fujita, W-H. Chen, D-Q. Yuan, Y. Nogami, T. Koga, T. Fujioka, K. Mihashi, S. Immel and F. W. Lichtenthaler, *Tetrahedron: Asymmetry*, 1999, **10**, 1689.
47 R. P. Bonomo, G. Maccarrone, E. Rizzarelli and G. Vecchio, *Inorg. Chim. Acta*, 2002, **339**, 455.
48 G. Maccarrone, E. Rizzarelli and G. Vecchio, *Polyhedron*, 2002, **21**, 1531.
49 G. Vecchio, T. Campagna, R. Marchelli and E. Rizzarelli, *J. Supramol. Chem.*, 2001, **1**, 117.
50 R. P. Bonomo, V. Cucinotta, G. Maccarrone, E. Rizzarelli and G. Vecchio, *J. Chem. Soc., Dalton Trans.*, 2001, 1366.
51 R. P. Bonomo, V. Cucinotta, F. D'Alessandro, G. Impellizzeri, G. Maccarrone, G. Vecchio and E. Rizzarelli, *Inorg. Chem.*, 1991, **30**, 2708.
52 R. P. Bonomo, V. Cucinotta, F. D'Alessandro, G. Impellizzeri, G. Maccarrone, E. Rizzarelli and G. Vecchio, *J. Inclusion Phenom. Mol. Recogn.*, 1993, **15**, 167.
53 R. P. Bonomo, V. Cucinotta, F. D'Alessandro, G. Impellizzeri, G. Maccarrone, E. Rizzarelli, G. Vecchio, L. Carima, R. Corradini, G. Sartor and R. Marchelli, *Chirality*, 1997, **9**, 341.
54 B. L. May, S. D. Kean, C. J. Easten and S. F. Lincoln, *J. Chem. Soc., Perkin Trans. 1*, 1997, 3157.
55 D. La Mendola, P. Mineo, E. Rizzarelli, E. Scamporrino, G. Vecchio and D. Vitalini, *J. Supramol. Chem.*, 2001, **1**, 147.
56 C. E. Brown, W. E. Antholine and W. Francisz, *J. Chem. Soc., Dalton Trans.*, 1980, 590.
57 J. F. Boas, J. R. Pilbrow, C. R. Hartzell and T. D. Smith, *J. Chem. Soc. A*, 1969, 572.
58 G. Brookes and L. D. Pettit, *J. Chem. Soc., Dalton Trans.*, 1975, 2112.
59 P. G. Daniele, E. Prenesti, V. Zelano and G. Ostacoli, *Spectrochim. Acta*, 1993, **49**, 1299.
60 J. Peisach and W. E. Blumberg, *Arch. Biochem. Biophys.*, 1974, **165**, 691.
61 E. W. Wilson, Jr., M. H. Kasperian and R. B. Martin, *J. Am. Chem. Soc.*, 1970, **92**, 5365.
62 D. Salvemini, D. P. Riley and S. Cuzzocrea, *Nature Rev., Drug Discov.*, 2002, **1**, 367.
63 J. R. J. Sorenson, *Prog. Med. Chem.*, 1989, **26**, 437.
64 G. Condorelli, L. L. Costanzo, G. De Guidi, S. Giuffrida, E. Rizzarelli and G. Vecchio, *J. Inorg. Biochem.*, 1994, **54**, 257.
65 S. Goldstein, C. Michel, W. Bors, M. Saran and G. Czapski, *Free Radical Biol. Med.*, 1988, **4**, 295.
66 D. Behar, C. Czapski, J. Rabani, L. M. Dorfman and H. A. Schwarz, *J. Phys. Chem.*, 1970, **74**, 3209.
67 J. Weinstein and B. H. J. Bielski, *J. Am. Chem. Soc.*, 1980, **102**, 4916.
68 C. Amar, E. Vilkas and J. Foss, *J. Inorg. Biochem.*, 1982, **17**, 313.
69 D. Klug-Roth, I. Fridovich and J. Rabani, *J. Am. Chem. Soc.*, 1973, **95**, 2786.
70 K. D. Asmun, M. Bonifacic, P. Toffel, P. O'Neill, D. Schulte-Frohlinde and S. Steenken, *J. Chem. Soc., Faraday Trans. I*, 1978, **74**, 1820.
71 G. V. Buxton and R. M. Sellers, *Coord. Chem. Rev.*, 1977, **22**, 195.
72 M. Tamba and A. Torreggiani, *Int. J. Radiat. Biol.*, 1998, **74**, 333.
73 F. Bosca, M. A. Miranda, G. Cardanico and D. Mauleon, *Photochem. Photobiol.*, 1994, **60**, 96.
74 S. Monti, S. Sortino, G. De Guidi and G. Marconi, *J. Chem. Soc., Faraday Trans.*, 1997, **93**, 2269.
75 S. Monti, S. Sortino, G. De Guidi and G. Marconi, *New J. Chem.*, 1998, 599.
76 G. De Guidi, G. Condorelli, S. Giuffrida, G. Puglisi and G. Giammona, *J. Inclusion Phenom.*, 1993, **15**, 43.
77 D. G. Nicholls and S. L. Budd, *Physiol. Rev.*, 2000, **80**, 315.
78 D. W. Choi, *J. Neurobiol.*, 1992, **23**, 1261.
79 D. W. Choi, *Cerebrovasc. Brain Metab. Rev.*, 1990, **2**, 105.
80 D. P. Riley, *Chem. Rev.*, 1999, **99**, 2573.
81 R. P. Bonomo, G. Impellizzeri, D. La Mendola, G. Maccarrone, G. Pappalardo, A. Santoro, G. Tabbì, G. Vecchio and E. Rizzarelli, in *Metal–Ligand Interactions in Molecular-, Nano- and Macro-systems in Complex Environments*, ed. N. Russo, D. R. Salahub and M. Witko, NATO ASI Series, Kluwer, Dordrecht, 2003, pp. 19–36.
82 J. S. Valentine and M. W. Pantoliano, in *Metal Ions in Biological System*, ed. H. Sigel, Dekker, New York, 1981, vol. 3, p. 291.
83 I. Bertini and S. Mangani, *Adv. Inorg. Chem.*, 1998, **45**, 127.